EUROFUSION WPMST2-PR(16) 16083

E. Hasan et al.

Electron energy distribution function in the divertor region of the COMPASS tokamak during neutral beam injection heating

Preprint of Paper to be submitted for publication in
Journal of Physics Conference Series

This work has been carried out within the framework of the EUROfusion Consortium and has received funding from the Euratom research and training programme 2014-2018 under grant agreement No 633053. The views and opinions expressed herein do not necessarily reflect those of the European Commission.

Electron energy distribution function in the divertor region of the COMPASS tokamak during neutral beam injection heating

E Hasan[1,2], M Dimitrova[2,3,5], J Havlicek[3], K Mitošinková[3,4], J Stöckel[3], J Varju[3], Tsv K Popov[1], M Komm[3], R Dejarnac[3], P Hacek[3,4], R Panek[3] and the COMPASS team

[1]Faculty of Physics, St. Kl. Ohridski University of Sofia,
5 J. Bourchier Blvd., 1164 Sofia, Bulgaria
[2]Acad. E. Djakov Institute of Electronics, Bulgarian Academy of Sciences,
72 Tsarigradsko Chaussee, 1784 Sofia, Bulgaria
[3]Institute of Plasma Physics, The Czech Academy of Sciences,
Za Slovankou 3, 182 00 Prague 8, The Czech Republic
[4]Faculty of Mathematics and Physics, Charles University in Prague,
Prague, The Czech Republic

E-mail: dimitrova@ipp.cas.cz

Abstract. This paper presents the results from swept probe measurements in the divertor region of the COMPASS tokamak in D-shaped, L-mode discharges, with toroidal magnetic field $B_T = -1.15$ T, plasma current $I_p = -180$ kA and line-average electron densities varying from 2 to 8×10^{19} m^{-3}. Using neutral beam injection heating, the electron energy distribution function (EEDF) is studied before and during the application of the beam.
The current-voltage characteristics data are processed using the novel first-derivative probe technique. This technique allows one to evaluate the plasma potential and the real EEDF (respectively, the electron temperatures and densities).
At the low average electron density of 2×10^{19} m^{-3}, the EEDF is bi-Maxwellian with a low-energy electron population with temperatures 4-6 eV and a high-energy electron group 12-25 eV. As the line-average electron density is increased, the electron temperatures decrease. At line-average electron densities above 7×10^{19} m^{-3}, the EEDF is found to be Maxwellian with a temperature of 6-8.5 eV.
The effect of the NBI heating power in the divertor region is also studied.

1. Introduction

The probe technique is frequently applied to diagnose the magnetized high-temperature strongly turbulent fusion edge plasmas. The knowledge of the real EEDF is of great importance in understanding the physics underlying the processes occurring in the magnetized plasma.

This paper presents the results from swept probe measurements in the divertor region of the COMPASS tokamak [1, 2] in D-shaped, L-mode additionally heated deuterium plasmas at $I_p = -180$ kA

[5] To whom any correspondence should be addressed.

and line-average electron densities varying from $n_e^{avr} = 2\times10^{19}$ m^{-3} to 8×10^{19} m^{-3}. The neutral beam injector (NBI) [3] injects the deuterium beam tangentially into the tokamak vessel in the same direction as the plasma current (co-injection). The energy of the beam is kept at $E_{NBI} = 40$ keV. The beam power P_{NBI} is varied by changing the value of the ion current extracted from the ion source I_{NBI} from ~200 kW ($I_{beam} = 6$ A) to ~320 kW ($I_{beam} = 10$ A). The plasma potential and the electron energy distribution function (EEDF) as obtained by using the first-derivative probe technique (FDPT) [4-7] are derived before and during the application of the beam power.

The dependence of the plasma potential and the EEDF on the NBI heating power is studied.

2. Langmuir probe measurements in the divertor region of the COMPASS tokamak

The divertor probe system in the COMPASS tokamak consists of 39 single graphite Langmuir probes poloidally embedded in the divertor tiles providing data with a 5 mm spatial resolution [5]. The probes are biased with respect to the tokamak chamber wall by a voltage U_p swept as triangular waveform at a frequency of 1 kHz supplied by a KEPCO 100-4M power supply. The probe bias and probe current are recorded by the COMPASS data acquisition system at a sampling frequency of 1 MHz. The current-voltage (*IV*) probe characteristics are constructed using the data recorded at different times before and during the NBI heating.

Further, the FDPT is applied to process the *IV* characteristics in order to obtain the plasma potential and the EEDF (respectively, the electron temperatures and densities) [4-7]. Figure 1 shows as an example two experimental *IV* characteristics from probe #10 (radial position $R = 0.4326$ m) before NBI heating at time $t = 1080$ ms, beginning of the discharge is at 970 ms. The *IV*s at $n_e^{avr} = 2\times10^{19}$ m^{-3} and $n_e^{avr} = 7\times10^{19}$ m^{-3} are presented by blue and black lines. Figure 2 presents (in both figures by red and green lines) the first derivative of the same *IV* curves and the fit with the model curves [8]. Using this comparison, one can evaluate the plasma potentials, which are 48 V and 26 V, respectively.

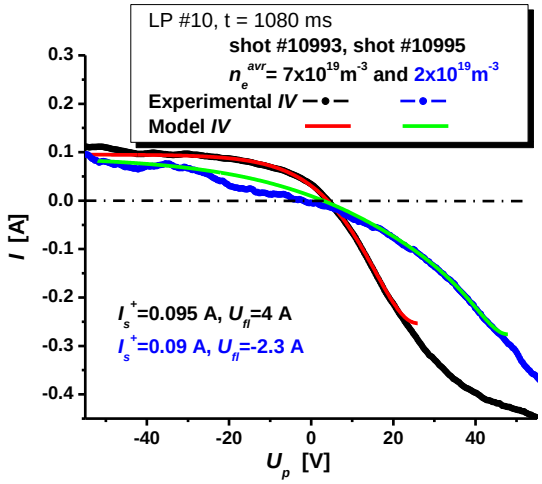

Figure 1. Current-voltage characteristics on probe #10 at $n_e^{avr} = 2\times10^{19}$ m^{-3} (blue line) and 7×10^{19} m^{-3} (black line) at a $t = 1080$ ms before NBI heating.

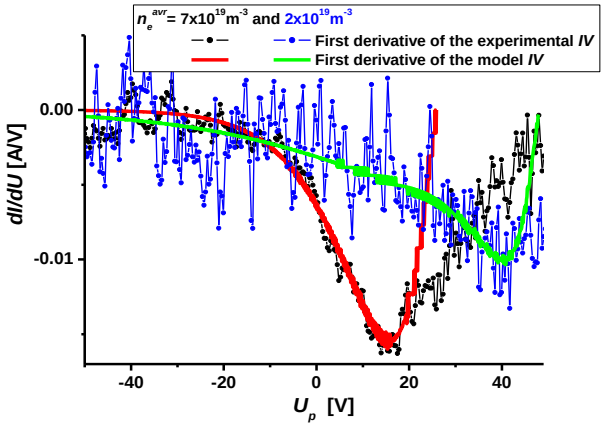

Figure 2. First derivatives of the experimental *IV* characteristics on probe #10 at $n_e^{avr} = 2\times10^{19}$ m^{-3} (blue) and $n_e^{avr} = 7\times10^{19}$ m^{-3} (black) and model curves, green and red curves respectively.

The corresponding electron energy probability functions (EEPF) [7] for both cases are plotted in figure 3. The EEPF provides the same information about the electron component as the EEDF and is frequently used to represent the probe data measured.

The EEPF, presented in a semi-log scale, allows a quick visualization of a departure of the measured EEPF from the Maxwellian distribution, which is a straight line in this representation [7]. Using the slope of the EEPF, one can determine the electron temperature.

It is seen that at $n_e^{avr} = 7\times10^{19}$ m^{-3} (black dots) EEPF can be approximated by a straight line (red). In this case we have a Maxwellian distribution with $T_e = (7.5\pm0.7)$ eV. In the case of $n_e^{avr} = 2\times10^{19}$ m^{-3} (blue dots), the electron distribution differs from the Maxwellian, but can be approximated by a bi-Maxwellian one, i.e., by a sum (the green line) of two distributions with two different temperatures: 4.5 eV (blue) and 18 eV (red dashed line). This is in agreement with our previous studies [5, 9].

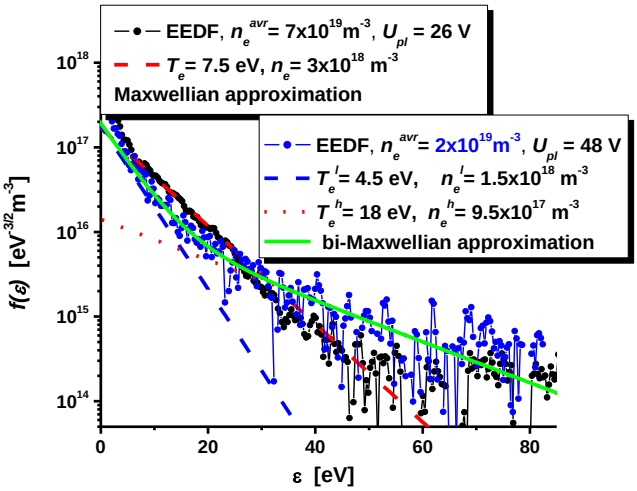

Figure 3. Experimental EEPF at 7×10^{19} m^{-3} (black dots), a Maxwellian distribution (red) at 2×10^{19} m^{-3} (blue dots) and a bi-Maxwellian distribution (green) - sum of the model ones for two electron temperatures for LP#10, $R = 0.4326$ m.

3. Results and discussion

We present the main plasma parameters estimated using the EEDF as derived from the *IV* characteristics before and during the application of the NBI. The results of determining the plasma potential's poloidal distribution and the electron temperatures are shown in figures 4 before a) and c) and during NBI heating (b) and d)), when the beam current is $I_{beam} = 6$ A. The different values of the line-average electron densities are indicated by different colors. The positions of the strike points (presented as regions) found from the reconstruction of the magnetic surfaces by the Equilibrium FITing code (EFIT) are also shown in all figures below.

It is seen that as the line-average electron density increases, the amplitude of the U_{pl} decreases. The difference in the values is strongly pronounced on the high-field side (HFS), where for $n_e^{avr} = 2\times10^{19}$ m^{-3} the plasma potential is $U_{pl} = 70$ V, while for $n_e^{avr} = 8\times10^{19}$ m^{-3} it is around $U_{pl} = 30$ V (figure 4 a)).

When the NBI is applied, the influence of the beam in the divertor is not too strong. A small increase in the range of a few volts for the U_{pl} is seen, better manifested at higher line-average electron densities. On the low field side (LFS) the change is bigger again for the higher line-average electron densities, but in a negative direction, the minima deepening (figure 4 b)). Concerning the election temperature when the line-average electron densities are varied, one a can see that at $n_e^{avr} = 2\times10^{19}$ m^{-3} the EEDF is bi-Maxwellian. When the density is increased to $n_e^{avr} = 6\times10^{19}$ m^{-3}, one finds that on the HFS and in the private flux region (PFR) the EEDF is Maxwellian. On the LFS it is again bi-Maxwellian. Above $n_e^{avr} = 7\times10^{19}$ m^{-3}, the EEDF is Maxwellian with a temperature 6-8.5 eV. The dependence of the NBI heating with $I_{beam} = 6$A is really weak: the electron temperature increases by few eV. The influence of the two-temperature EEDF on the parallel heat flux density, as well as a discussion on the origin of the bi-Maxwellian EEDF, are presented in detail in our recent publication [6].

The electron density is calculated using the expression for normalization of the EEDF [4]. In figure 5, an example is given of the poloidal distribution of the electron densities as determined using the FDPT. The case of a bi-Maxwellian EEDF corresponds to the low line-average density $n_e^{avr} = 2\times10^{19}$ m^{-3} (figure 5 a). The low-temperature electron group (blue triangles, $T_e^l = 4\pm0.4$ eV) has a density similar or higher than the high-temperature one (red squares, $T_e^h = 12\text{-}25\pm0.2$ eV). At $n_e^{avr} = 6\times10^{19}$ m^{-3} (figure 5 b) on the HFS and in the private flux region (PFR), the EEDF is Maxwellian. On the LFS it is bi-Maxwellian. This peculiarity is not affected by the NBI heating.

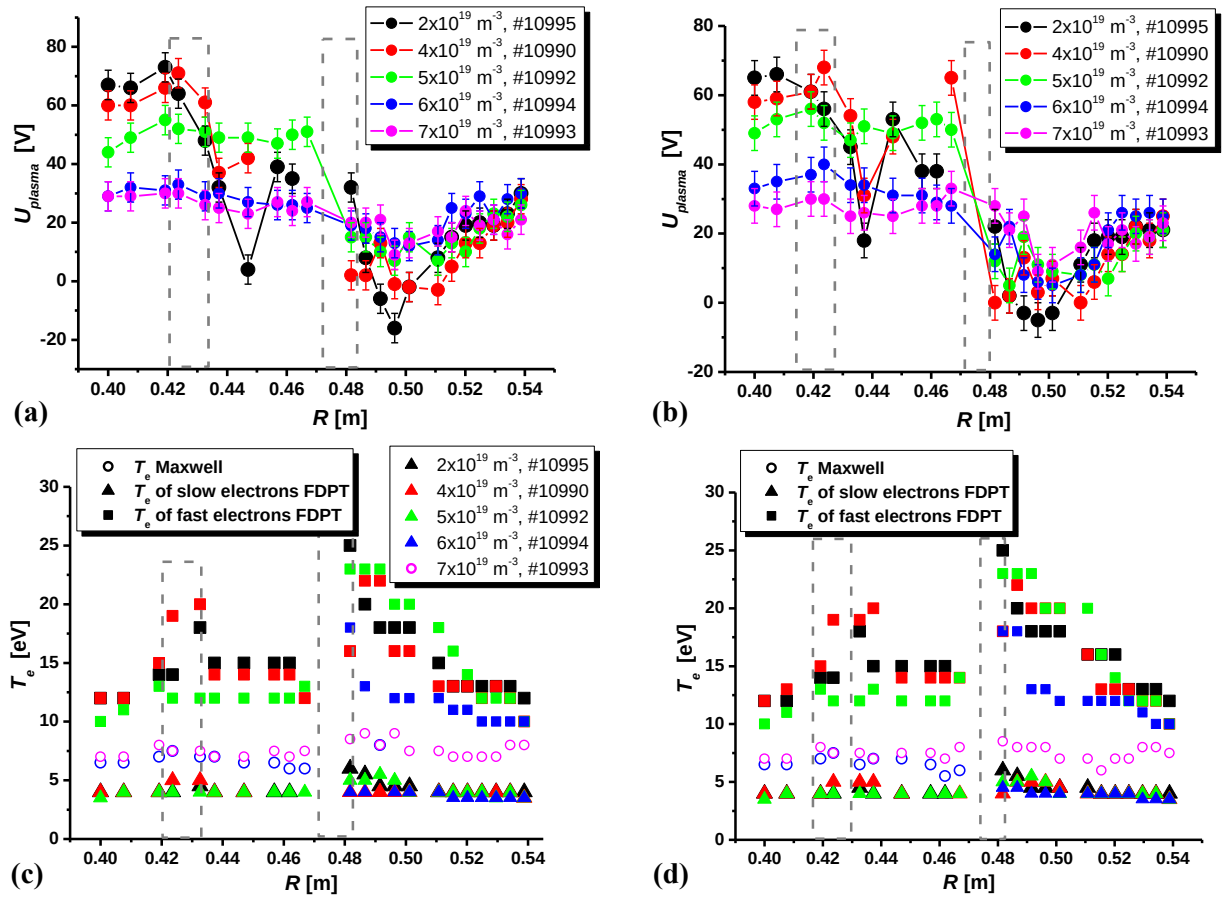

Figure 4 . Poloidal distribution of the plasma potential **a)** before and **b)** during I_{beam} =6 A NBI and the electron temperatures **c)** before and **d)** during NBI.

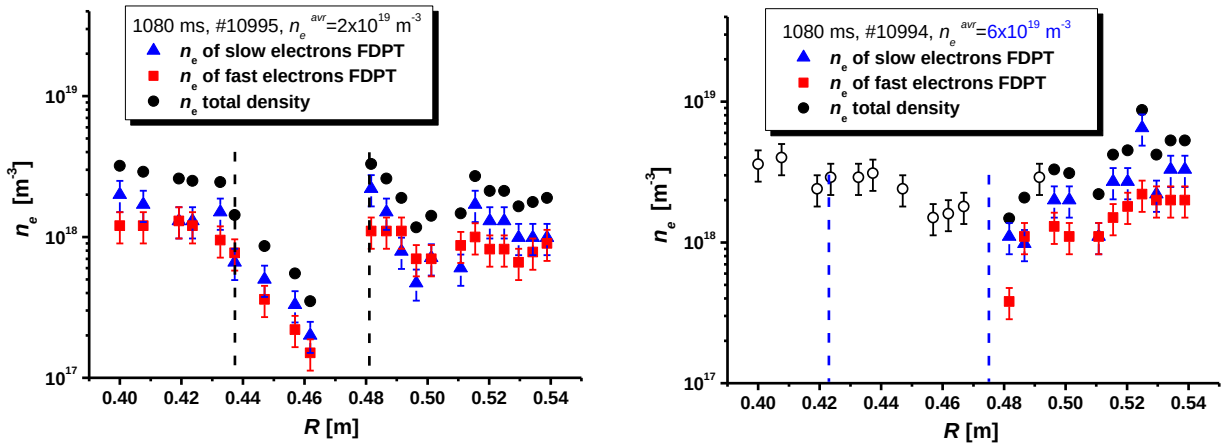

Figure 5 . Poloidal distribution of the electron density at **a)** $n_e^{avr} = 2\times10^{19}$ m^{-3} and **b)** $n_e^{avr} = 6\times10^{19}$ m^{-3} before NBI heating.

The weak effect at I_{beam} = 6 A can be explained by the fact that at values below 10 A the divergence of the neutral beam is rather high and a significant fraction of the neutral beam power is lost in a relatively narrow beam duct connecting NBI with the tokamak vessel.

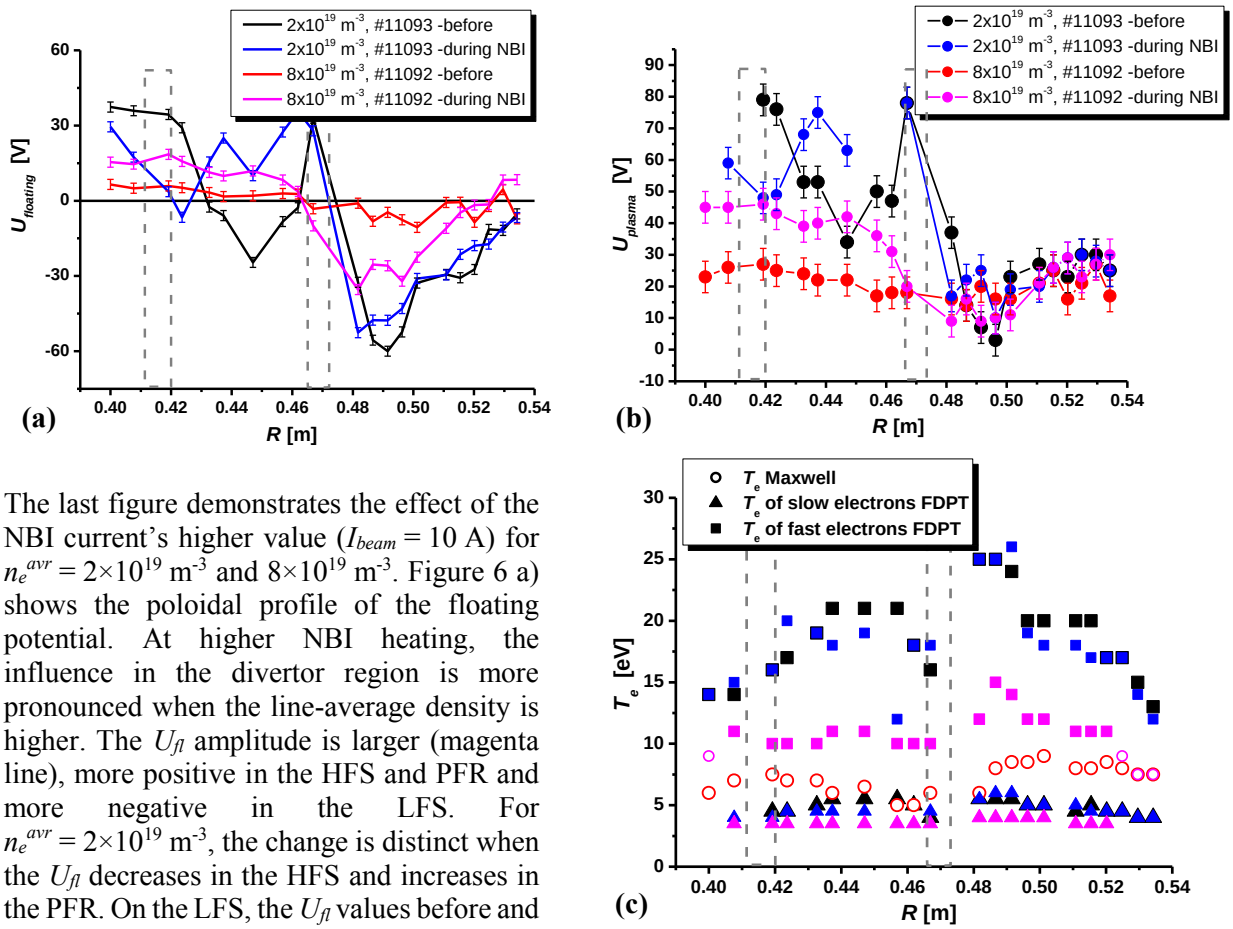

Figure 6. Poloidal distribution of the **a)** floating potential, **b)** plasma potential and **c)** the electron temperature for two values of the line-average density, before and during NBI heating.

The last figure demonstrates the effect of the NBI current's higher value (I_{beam} = 10 A) for $n_e^{avr} = 2\times10^{19}$ m^{-3} and 8×10^{19} m^{-3}. Figure 6 a) shows the poloidal profile of the floating potential. At higher NBI heating, the influence in the divertor region is more pronounced when the line-average density is higher. The U_{fl} amplitude is larger (magenta line), more positive in the HFS and PFR and more negative in the LFS. For $n_e^{avr} = 2\times10^{19}$ m^{-3}, the change is distinct when the U_{fl} decreases in the HFS and increases in the PFR. On the LFS, the U_{fl} values before and during NBI are almost the same. The behavior of the plasma potential profile (figure 6 b)) is similar in the HFS and the PFR; however, in the LFS the values of U_{pl} do not change significantly without any dependence on the density and the NBI heating power.

The poloidal profile of the electron temperatures is presented in figure 6 c). It is seen that at a lower line-average density, the temperatures remain almost the same. For $n_e^{avr} = 8\times10^{19}$ m^{-3} before the additional heating, the EEDF is Maxwellian (red empty dots). During the heating by a higher power, which increases the electron temperature, a bi-Maxwellian distribution appears (magenta symbols).

4. Conclusions

This paper reports the results from swept probe measurements in the divertor region of the COMPASS tokamak with a plasma current of I_p = - 180 kA and line-average electron densities varying from 2 to 8×10^{19} m^{-3}. Using neutral beam injection heating, the electron energy distribution function is studied before and during the application of the beam.

The EEDF and the other plasma parameters in the divertor of the COMPASS tokamak are determined by the first-derivative probe technique.

At a low line-average electron density (2×10^{19} m^{-3}), the EEDF is bi-Maxwellian with a low-energy electron population with temperatures 4-6 eV and a high-energy electron group (12-25 eV). Raising the line-average electron density leads to a decrease in the electron temperatures. Above $n_e^{avr} = 7\times10^{19}$ m^{-3}, the EEDF is found to be Maxwellian with a temperature 6-8.5 eV.

The effect of NBI heating in the divertor region is more pronounced at values higher than I_{beam} = 10 A.

Acknowledgements
This research has been partially supported by the Joint Research Project between the Institute of Plasma Physics of the CAS and the Institute of Electronics BAS BG, by the Czech Science Foundation grant GA16-25074S, by MSMT project # LM2015045 and by the Co-fund under MEYS project # 8D15001. This work has been carried out within the framework of the EUROfusion Consortium and has received funding from the Euratom research and training programme 2014-2018 under grant agreement No 633053. The views and opinions expressed herein do not necessarily reflect those of the European Commission.

References
[1] Panek R, et al 2015 *Plasma Phys. Control. Fusion* **58** 014015
[2] Weinzettl V, et al 2011 *Fusion Engineering and Design* **86** 1227–1231
[3] Deichuli P et al 2012 *Rev. Sci. Instrum*. **83** 02B114
[4] Popov Tsv K, Ivanova P I, Stockel J and Dejarnac R 2009 *Plasma Phys. Control. Fusion* **51** 065014
[5] Dimitrova M, Dejarnac R, Popov Tsv K, Ivanova P, Vasileva E, Kovačič J, Stöckel J, Havlicek J, Janky F and Panek R 2014 *Contrib. Plasma Phys*. **54** No. 3 255–60
[6] Popov Tsv K, et al 2015 *Plasma Phys. Control. Fusion* **57** 115011
[7] Popov Tsv K et al 2016 *Plasma Sources Sci. Technol*. **25** 033001
[8] Popov Tsv K et al 2014 *Contrib. Plasma Phys.* **54** No. 3 267272
[9] Ivanova P, Dimitrova M, Vasileva E, Popov Tsv K, Dejarnac R, Stöckel J, Imríšek M, Hacek P and Panek R 2016 *J. Phys.: Conf. Series* (6th Int. Workshop & Summer School on Plasma Phys. 2014, Kiten, Bulgaria), in press